Polymer Chemistry

PAPER

Cite this: *Polym. Chem.*, 2019, **10**, 345

Synthesis, characterization and electrochromic properties of novel redox triarylamine-based aromatic polyethers with methoxy protecting groups†

Jung-Tsu Wu, ‡[a] Yang-Ze Fan‡[a] and Guey-Sheng Liou *[a,b]

Received 9th September 2018,
Accepted 24th November 2018

DOI: 10.1039/c8py01308j

rsc.li/polymers

Five novel triphenylamine derivatives with two silyl ether protecting groups were readily synthesized and further underwent silyl polycondensation to obtain novel electro-active aromatic polyethers. These polymers exhibited high optical transparency, were colourless, were soluble in many organic solvents, and had useful levels of thermal stability associated with moderately high glass-transition temperatures and char yields. These anodically polymeric electrochromic materials displayed highly reversible electrochemical and electrochromic behaviour, with interesting and useful multi-colour changes related to their different oxidation stages.

Introduction

Chromism relates to the colour change of materials caused by outside stimulus, and electrochromism is interesting behaviour exhibited by electroactive species where different colours can be produced by oxidized and reduced states during electrochemical processes. In 1961, Platt first reported the electrochromic (EC) phenomenon;[1] then, Deb used amorphous WO_3 thin film to make a sandwich type EC device (ECD) in 1969.[2] In recent years, because of the great potential of this phenomenon, products generated incorporating this feature have gradually emerged in our life, such as smart windows,[3] sunglasses,[4] and so on. Thus, multitudinous EC materials have been developed and most studies have concentrated on ameliorating their properties. Such materials can be sorted into five major categories: metal oxides;[5] coordination complexes;[6] small organic molecules;[7–9] conjugated polymers;[10–13] and arylamine-based polymers.[14,15] EC materials containing triphenylamine (TPA) units possess remarkable colour transitions, and have been investigated to understand underlying methods for augmenting the stages of colour change.[16–18] First and foremost, EC moieties with two or more TPA units can be introduced into polyimides and polyamides to obtain multiple oxidation redox stages in order to mingle and generate multifarious colours.[19,20] Our group has been working on triarylamine-based polymers since 2012 based on these approaches, and plenty of excellent EC materials with TPA units have been developed successfully, like polyimides,[21] polyamides,[22] epoxies[23] and polybenzoxazines.[24] All these types of materials show interesting colour transitions with desirable EC reversibility in the visible region. Furthermore, it is worth noting that the significant advantages of these types of EC polymer thin films are the high transparencies and that they are almost colourless in the neutral state without any burden of applied potential.[25]

Aromatic polyether is also a well-known high-performance polymer, having higher transparency and better colourless characteristics than other structurally related polymers such as polyamides and polyimides. We have also prepared some polyethers with TPA units, such as poly(ether sulfone) (**PES**) and poly(ether oxadiazole) (**PEOX**) examples, however the resulting polymers could not display excellent electrochemical stability owing to the unprotected para-position of the TPA units, which undergo intermolecular coupling reactions. Hence, such materials could only be used for other applications, such as polymer memory.[26] In order to prevent two cationic radicals ($TPA^{+\bullet}$) from coupling tail to tail, the introduction of electron-donating methoxy groups at the para-position of the phenyl rings should be an effective approach. However, hydroxy and methoxy groups are very difficult to obtain simultaneously in the same molecule *via* simple synthesis reactions, and the obtained triarylamine-based diphenol monomers with methoxy substituents are always hard to purify to a high purity

[a]*Institute of Polymer Science and Engineering, National Taiwan University, 10607 Taipei, Taiwan. E-mail: gsliou@ntu.edu.tw*
[b]*Advanced Research Center for Green Materials Science and Technology, National Taiwan University, 10607 Taipei, Taiwan*

†Electronic supplementary information (ESI) available: Full experimental information, including details of the experimental section, data analysis, and supporting figures and tables. See DOI: 10.1039/c8py01308j

‡These authors equally contributed to this work.

for polymer synthesis. In addition, to obtain monomers with hydroxy and methoxy groups, silyl ether groups are also a judicious choice, and can further undergo deprotection to produce hydroxy groups. Furthermore, an interesting method, a 'silyl reaction', reported by Kricheldorf in 1983 could also be used to prepare polyethers.[27] The silyl ether groups could react directly with activated aromatic dichlorides or difluorides to generate the corresponding aromatic polyethers, indicating that pre-deprotection and purification after obtaining diphenol monomers will be not necessary when using the silyl reaction approach. Consequently, we hence utilize this unique type of polycondensation reaction to prepare nine novel electroactive aromatic polyethers (**TPA-PES**, **TPPA-PES**, **STPPA-PES**, **TPB-PES**, **BDATPA-PES**, **TPA-PEOX**, **TPPA-PEOX**, **TPB-PEOX** and **BDATPA-PEOX**) from five electroactive TPA based monomers with two para-silylether groups (four new compounds) and bis(4-fluorophenyl)sulfone or 2,5-bis(4-fluorophenyl)-1,3,4-oxadiazole. The general properties, such as the solubility, thermal properties and electrochemical behaviour, of the resulting polyether films were investigated. The synthesized polymers exhibited outstanding thermal stability, as expected, because of their wholly aromatic structures. In addition, the incorporation of an ether linkage also could enhance the solubility and transparency of the resulting polymers. Furthermore, these redox-active polyethers revealed excellent electrochemical stability and interesting multi-coloured EC behaviour.

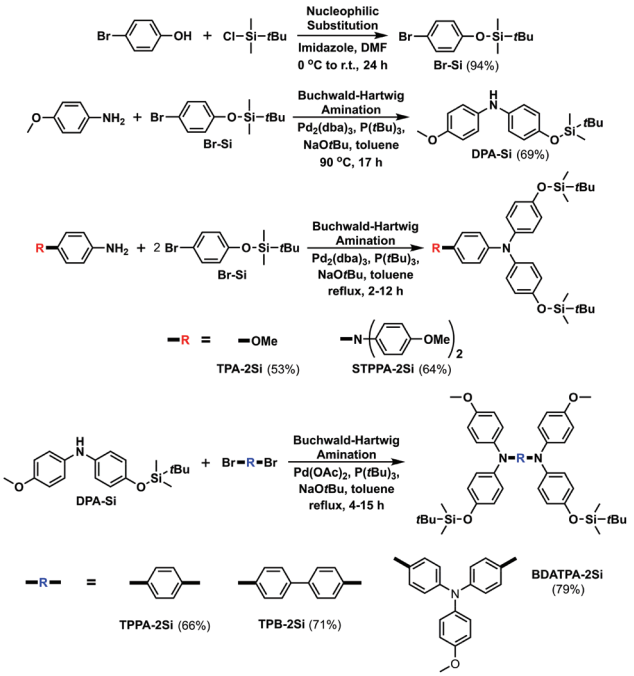

Scheme 1 Synthesis routes for the monomers.

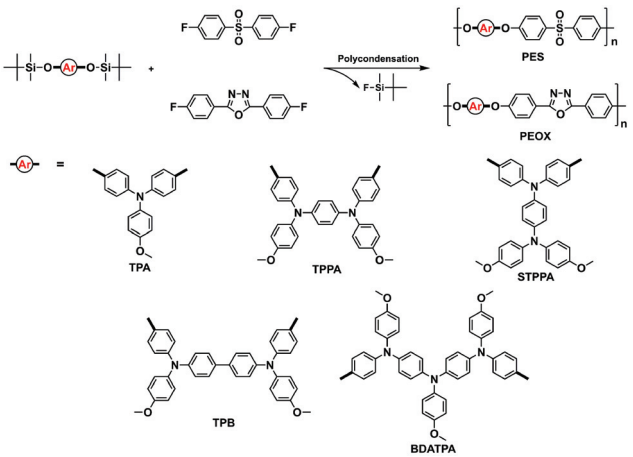

Scheme 2 Synthesis routes for the polymers.

Results and discussion

Monomer synthesis and characterization

Colourless **Br-Si** liquid was first synthesized from 4-bromophenol following the previous literature.[28] **DPA-Si**, an important intermediate product, was obtained using Buchwald–Hartwig amination with a yield of 69%. Then, three final products, **TPPA-2Si**, **TPB-2Si** and **BDATPA-2Si**, with yields higher than 65% were synthesized *via* the same procedure. The NMR spectra of **Br-Si**, **DPA-Si** and **TPB-2Si** displayed good agreement with the literature, as shown in Fig. S1–S3.†[28–30]

After this, the other compounds are new compounds, and their NMR spectra are summarized in Fig. S4–S11.† The other new compounds, **TPA-2Si** and **STPPA-2Si**, were obtained directly through the reaction of *p*-anisidine or **TPA-NH$_2$** with **Br-Si** by means of Buchwald–Hartwig amination, and their NMR spectra are depicted in Fig. S12–S19.† All of the synthesis routes are summarized in Scheme 1.

Polymer synthesis and basic properties

Two types of polyethers, **PES** and **PEOX**, were successfully prepared *via* silyl method polycondensation, as shown in Scheme 2. The silyl ether groups were first deprotected using CsF, and the resulted phenoxide salt could further undergo an S_N2 reaction with two kinds of difluoride monomers to produce two polyether series. The inherent viscosities, molecular weights and solubility behavior of the obtained polyethers are summarized in Tables S1 and S2.† The resulting polyethers with moderately high molecular weights exhibited good solubility in various organic solvents, and flexible and transparent polyether films could be obtained *via* solution-casting except in the case of **STPPA-PES**, as shown in Fig. S20.† The thermal properties of these polymers were investigated *via* TGA (Fig. S21†) and DSC (Fig. S22†), and the results are summarized in Table S3.† All the prepared aromatic polyethers exhibited good thermal stability without significant weight loss up to 400 °C under nitrogen and air atmospheres. The carbonized residues (char yields) of these TPA-based polyethers were in the range of 50–60% at 800 °C under a nitrogen atmosphere. The glass-transition temperatures (T_g) of these polymers were around 200 °C, except for the TPB series where they

were around 220 °C. FT-IR spectra of the **PES** examples are illustrated in Fig. S23;† two obvious characteristic absorption changes can be found in the region of 2900–3200 and 600–750 cm^{-1}, one for C–H and one for C–S stretching, respectively. On the other hand, C=N stretching of the oxadiazole group for the **PEOX** examples can be found at around 1600 cm^{-1} in Fig. S24.† 1H NMR spectra of these polymers were also recorded and are depicted in Fig. S25–S33.† All the signals from silylether groups (0–1.0 ppm) in these polymers disappeared, while the hydrogen peaks near the sulfone and oxadiazole electron withdrawing groups could be found at the same place as in the original starting monomers (~8.00 ppm).

Electrochemistry of the monomers

Firstly, the electrochemical oxidation redox behaviour of the three monomers was investigated *via* differential pulse voltammetry using an optically transparent thin-layer electrochemical cell in dehydrated acetonitrile (MeCN) or *N*-methyl-2-pyrrolidone, containing a 1 mM concentration of electrochromic material and 0.1 M tetrabutylammonium tetrafluoroborate ($TBABF_4$) as the supporting electrolyte under a nitrogen atmosphere for oxidation measurements. The results of the electrochemical measurements for these monomeric materials revealed one to three oxidation stages related to the quantity of electro-active nitrogen centre present, as illustrated in Fig. S34.†

Electrochemistry of the polymers

The electrochemical properties of the polyethers with TPA units, **PES** and **PEOX** examples, were investigated *via* cyclic voltammetry, conducted using cast film on an ITO-coated glass substrate as the working electrode in MeCN containing 0.1 M $TBABF_4$ as an electrolyte under a nitrogen atmosphere during the oxidation redox measurements. Typical cyclic voltammograms are illustrated in Fig. 1 and summarized in Table S4.† Interestingly, **STPPA-PES** exhibits a lower oxidation potential peak at 0.68 V than the isomeric **TPPA-PES** (0.82 V), as shown in Fig. 1a, due to the nitrogen centre on the pendent side of the STPPA structure having two electron-donating methoxy groups, while the two nitrogen centres on both sides have the same donor ability in **TPPA-PES**. Besides, the oxidation potentials of **TPB-PES** in the first and second states are closer than those of **TPPA-PES**, implying that the longer biphenyl bridge distance reduces the coupling effect of the cationic radical of $N^{+\bullet}$ in the first oxidation state on the other neutral N within the TPB moiety. Thus, it demonstrates a similar oxidation potential to **TPA-PES**. For **TPA-**, **TPPA-** and **BDATPA-PES**, the oxidation potential of the first oxidation state decreased obviously upon increasing the active nitrogen centres. A similar relationship could also be observed in the **PEOX** series. In addition, the electrochemical behaviour of the acceptor moieties in the ambipolar polyethers was investigated using **BDATPA-PES** and **BDATPA-PEOX** as a comparison model, and the results are depicted in Fig. S35.† The reduction potential for **BDATPA-PES** is −1.96 V, higher than −1.74 V for **BDATPA-PEOX** owing to the stronger electron-withdrawing capability of the oxadiazole moiety.

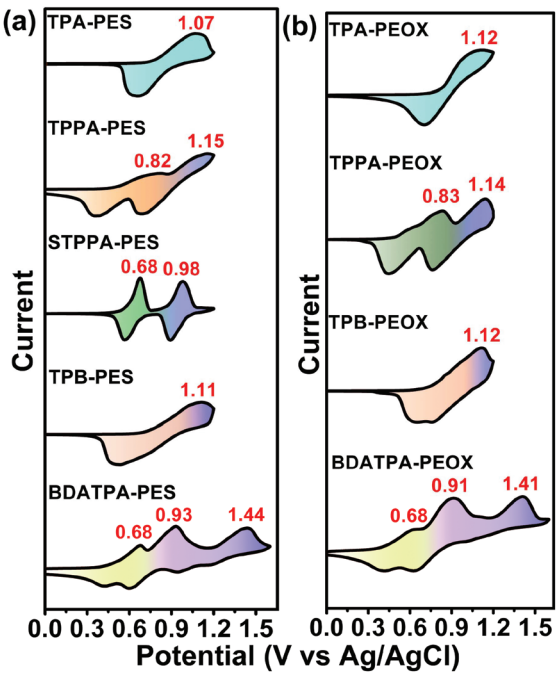

Fig. 1 Cyclic voltammograms of (a) **PES** and (b) **PEOX** polymer films on ITO-coated glass substrates in MeCN containing 0.1 M $TBABF_4$ at a scan rate of 50 mV s^{-1}.

Spectroelectrochemistry of the polymers

The spectroelectrochemical properties of these polyethers were studied *via* UV-vis spectroscopy coupled with a quartz cell containing an electrode. The electrode preparation and solution conditions were identical to those used for CV measurements.

Absorption spectra and L*a*b* CIE values for each corresponding oxidation state of the **PES** series are illustrated in Fig. 2. First, the colour of **TPA-PES** changed from colourless to a cyan colour when the applied potential increased positively from 0.00 to 1.00 V; the absorption peak at 738 nm grew intensely, as shown in Fig. 2a and f. For **TPPA-PES**, the colour changed from colourless to a light brown colour as the applied potential increased positively from 0.00 to 0.70 V, related to the first oxidation stage. The characteristic absorption peak at 326 nm decreased gradually while three new peaks arose at 413, 557, and 957 nm (a broad inter-valence charge transfer (IV-CT) absorption band in the NIR region).[31] When the potential was adjusted to a more positive value of 1.00 V, corresponding to the second oxidation state, the peaks at 413 and 957 nm decreased immediately while two new peaks arose at 584 and 768 nm, resulting in a blue colour, as depicted in Fig. 2b and g. Afterwards, the characteristic peak for **STPPA-PES** at 308 nm decreased gradually while three new peaks arose at 414, 585 and 987 nm when a potential was applied relating to the first oxidation state. Also, the absorption shape and peaks are different to those of **TPPA-PES**,

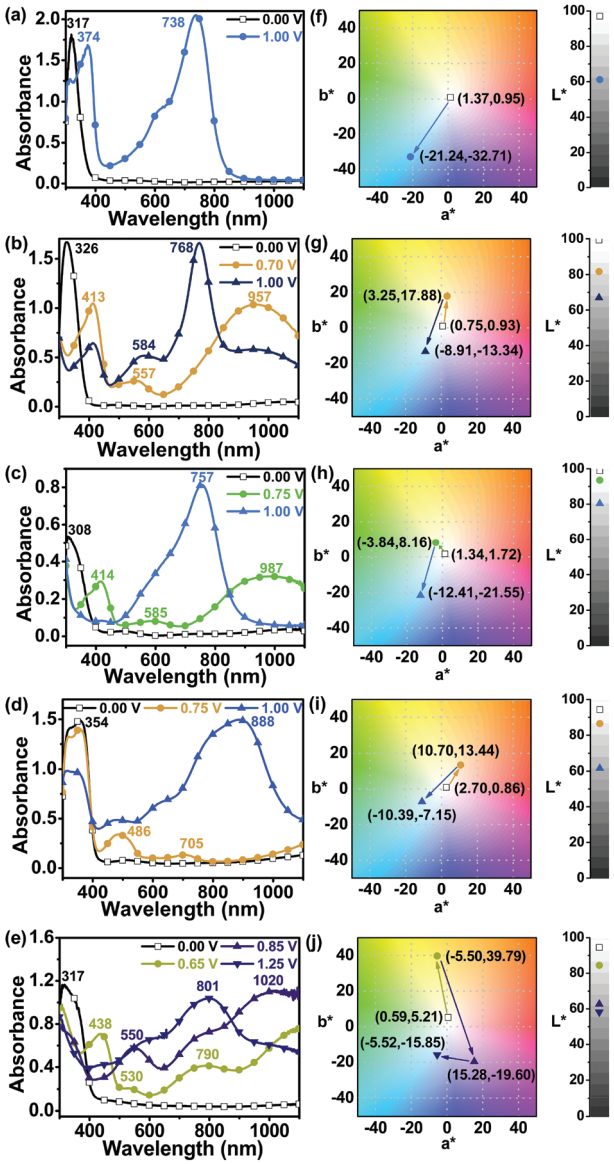

Fig. 2 Absorbance spectra and L*a*b* CIE data for (a, f) **TPA-PES** (400 ± 50 nm), (b, g) **TPPA-PES** (500 ± 50 nm), (c, h) **STPPA-PES** (220 ± 60 nm), (d, i) **TPB-PES** (500 ± 60 nm), and (e, j) **BDATA-PES** (500 ± 60 nm) film on ITO-coated glass substrates in MeCN containing 0.1 M $TBABF_4$ at applied potentials (V *vs.* Ag/AgCl) related to the different oxidation states.

resulting in different colour changes, from colourless to a green colour. When the potential was adjusted to 1.00 V, corresponding to the second oxidation state, the peaks at 414 nm and 987 nm decreased while a new peak arose at 757 nm with a shoulder at around 600 nm, and it became a sky blue colour, as shown in Fig. 2c and h. For **TPB-PES**, the peak of the characteristic absorption in the UV region decreased gradually, while three new peaks arose – at 486 and 705 nm and an IV-CT broad band – when the potential increased positively from 0.00 to 0.75 V, and the colour changed from colourless to a light orange colour. Then, the potential was adjusted to 1.00 V, corresponding to the second oxidation state; a broad absorption band over the visible light region with a peak at 888 nm was observed, and the colour changed to a blue colour, as depicted in Fig. 2d and i. Furthermore, **BDATPA-PES** demonstrates valuable three-stage multi-coloured changes. The peak of the characteristic absorption at 317 nm decreased gradually, while four new peaks grew up – at 438, 530 and 790 nm, and an IV-CT band with a colour change from colourless to a yellow green colour – when the applied potential increased positively from 0.00 to 0.65 V. When the potential was adjusted to 0.85 V, corresponding to the second oxidation state, the absorption peak at 438 nm decreased while the peak at 530 nm and the IV-CT broad band were enhanced and shifted to 550 nm and 1020 nm, respectively, and the colour of the film became purple. For the final oxidation state, a broad band with a peak at 801 nm could be observed and the colour changed to a deep blue colour, as shown in Fig. 2e and j.

Interestingly, besides **TPA-PES**, other polyethers such as **TPPA-PES**, **STPPA-PES**, **TPB-PES**, and **BDATPA-PES** revealed an IV-CT band in the first oxidation stage, and also in the second stage for **BDATPA-PES** with more electroactive nitrogen centres. Meanwhile, absorption spectra and L*a*b* CIE data for each related oxidation state for another similar series, **PEOX**, are summarized in Fig. S36.† The electrochromic behaviour is also described in the ESI,† and photographs of the colour changes at different oxidation states for these two series of polyethers were also taken, and the results are depicted in Fig. 3 and Fig. S37.†

Furthermore, the optical transparency and oxidation potential of the obtained aromatic polyethers were compared with polyimides[32] and polyamides[33] with the same triarylamine

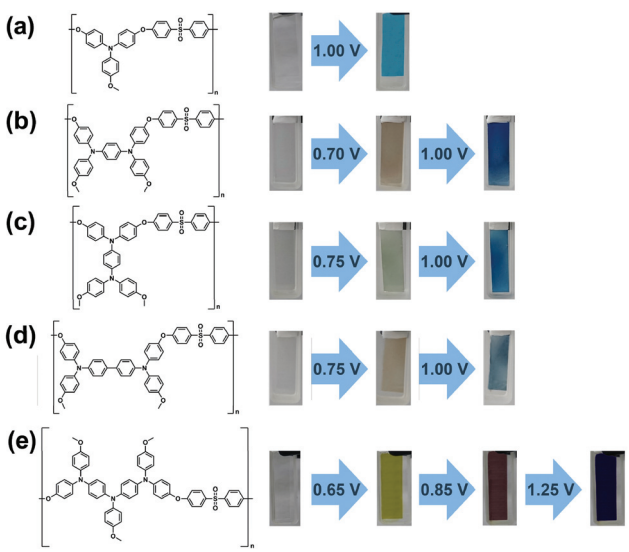

Fig. 3 Electrochromic behaviour of sulfone-type polyether films with thicknesses of (a) 650 ± 50, (b) 650 ± 50, (c) 500 ± 50, (d) 450 ± 50, and (e) 700 ± 50 nm on ITO-coated glass in MeCN containing 0.1 M $TBABF_4$ at applied potentials (V *vs.* Ag/AgCl) related to different oxidation states.

structures that have been published by our group previously. For instance, **BDATPA-PES** film exhibited lower oxidation potentials (0.65, 0.85 and 1.25 V) for all three oxidation states than the corresponding **BDATPA-PI** (0.70, 1.05 and 1.40 V). In addition, these polyether films also demonstrated higher transparency and colourlessness in the neutral state than the corresponding polyamides and polyimides, demonstrating the additional merit of isolated ether linkages in the polyether backbones.

Conclusions

In conclusion, a series of TPA derivatives and their corresponding novel aromatic polyethers have been readily prepared *via* silyl polycondensation reactions. The resulting polymers exhibited good thermal stability and solubility in many solvents due to the bulky triarylamine units and ether linkages. These electroactive polyether films displayed multi-coloured EC behaviour, from their original colourless neutral forms to different colours in related oxidation states. Furthermore, thanks to the optical advantages of polyethers, the film thickness could be increased to enhance the colour contrast in the switching state without sacrificing transparency and colourlessness in the original neutral state; this is because charge transfer generated *via* the donor-accepter effect could be greatly supressed by the ether linkage compared to the corresponding polyimides. Based on these results, these polyethers may be diamonds in the rough regarding electrochromic applications.

Conflicts of interest

There are no conflicts to declare.

Acknowledgements

This work was financially supported by the "Advanced Research Center for Green Materials Science and Technology" of the Featured Area Research Center Program within the framework of the Higher Education Sprout Project by the Ministry of Education (107L9006) and the Ministry of Science and Technology in Taiwan (MOST 107-3017-F-002-001 and 104-2113-M-002-002-MY3).

Notes and references

1 J. R. Platt, *J. Chem. Phys.*, 1961, **34**, 862.
2 S. K. Deb, *Appl. Opt.*, 1969, **8**, 192.
3 C. G. Granqvist, M. A. Arvizu, İ. B. Pehlivan, H. Y. Qu, R. T. Wen and G. A. Niklasson, *Electrochim. Acta*, 2018, **259**, 1170.
4 A. M. Österholm, D. E. Shen, J. A. Kerszulis, R. H. Bulloch, M. Kuepfert, A. L. Dyer and J. R. Reynolds, *ACS Appl. Mater. Interfaces*, 2015, **7**, 1413.
5 W. C. D. Smith, *Displays*, 1982, **3**, 3.
6 D. M. DeLongchamp and P. T. Hammond, *Adv. Funct. Mater.*, 2014, **14**, 224.
7 D. Weng, Y. C. Shi, J. M. Zheng and C. Y. Xu, *Org. Electron.*, 2016, **34**, 139.
8 D. C. Huang, J. T. Wu, Y. Z. Fan and G. S. Liou, *J. Mater. Chem. C*, 2017, **5**, 9370.
9 J. T. Wu and G. S. Liou, *Chem. Commun.*, 2018, **54**, 2619.
10 W. Lu, A. G. Fadeev, B. H. Qi, E. Smela, B. R. Mattes, J. Ding, G. M. Spinks, J. Mazurkiewicz, D. Z. Zhou, G. G. Wallace, D. R. MacFarlane, S. A. Forsyth and M. Forsyth, *Science*, 2002, **297**, 983.
11 P. M. Beaujuge and J. R. Reynolds, *Chem. Rev.*, 2010, **110**, 268.
12 W. T. Neo, Q. Ye, S. J. Chua and J. W. Xu, *J. Mater. Chem. C*, 2016, **4**, 7364.
13 Y. J. Hu, D. F. Hu, S. L. Ming, X. M. Duan, F. Zhao, J. Hou, J. K. Xu and F. X. Jiang, *Electrochim. Acta*, 2016, **189**, 64.
14 S. Beaupre, J. Dumas and M. Leclerc, *Chem. Mater.*, 2006, **18**, 4011.
15 H. J. Yen and G. S. Liou, *Polym. Chem.*, 2018, **9**, 3001.
16 M. Y. Chou, M. K. Leung, Y. L. O. Su, C. L. Chiang, C. C. Lin, J. H. Liu, C. K. Kuo and C. Y. Mou, *Chem. Mater.*, 2004, **16**, 654.
17 J. Natera, L. Otero, F. D'Eramo, L. Sereno, F. Fungo, N. S. Wang, Y. M. Tsai and K. T. Wong, *Macromolecules*, 2009, **42**, 626.
18 F. B. Koyuncu, S. Koyuncu and E. Ozdemir, *Electrochim. Acta*, 2010, **55**, 4935.
19 S. H. Cheng, S. H. Hsiao, T. X. Su and G. S. Liou, *Macromolecules*, 2005, **38**, 307.
20 C. W. Chang and G. S. Liou, *J. Mater. Chem.*, 2008, **18**, 5638.
21 H. J. Yen, C. J. Chen and G. S. Liou, *Adv. Funct. Mater.*, 2013, **23**, 5307.
22 H. S. Liu, B. C. Pan, D. C. Huang, Y. R. Kung, C. M. Leu and G. S. Liou, *NPG Asia Mater.*, 2017, **9**, e388.
23 Y. W. Chuang, H. J. Yen, J. H. Wu and G. S. Liou, *ACS Appl. Mater. Interfaces*, 2014, **6**, 3594.
24 L. C. Lin, H. J. Yen, C. J. Chen, C. L. Tsai and G. S. Liou, *Chem. Commun.*, 2014, **50**, 13917.
25 H. J. Yen and G. S. Liou, *Polym. Chem.*, 2018, **9**, 3001.
26 C. J. Chen, Y. C. Hu and G. S. Liou, *Polym. Chem.*, 2013, **4**, 4162.
27 H. R. Kricheldorf and G. Bier, *J. Polym. Sci., Part A: Polym. Chem.*, 1983, **21**, 2283.
28 R. J. Edsall, H. A. Harris, E. S. Manas and R. E. Mewshaw, *Bioorg. Med. Chem.*, 2003, **11**, 3457.
29 P. Casara, T. L. Diguarher, J. M. Henlin, J. B. Starck, A. L. Tiran, G. D. Nanteuil, O. Geneste, J. E. P. Davidson, J. B. Murray, I. J. Chen, C. Walmsley, C. J. Graham, S. Ray, D. Maddox and S. Bedford, *LES LABORATOIRES SERVIER, FR.*, VERNALIS R&D LTD., FR3008978A1, 2015.

30 C. Carter, M. Brumbach, C. Donley, R. D. Hreha, S. R. Marder, B. Domercq, S. Yoo, B. Kippelen and N. R. Armstrong, *J. Phys. Chem. B*, 2006, **110**, 25191.
31 A. V. Szeghalmi, M. Erdmann, V. Engel, M. Schmitt, S. Amthor, V. Kriegisch, G. Nöll, R. Stahl, C. Lambert, D. Leusser, D. Stalke, M. Zabel and J. Popp, *J. Am. Chem. Soc.*, 2004, **126**, 7834.
32 L. T. Huang, H. J. Yen and G. S. Liou, *Macromolecules*, 2011, **44**, 9595.
33 G. S. Liou and H. Y. Lin, *Macromolecules*, 2009, **42**, 125.

